

Exploring the Conformational and Biological Versatility of β -Turn-Modified Gramicidin S by Using Sugar Amino Acid Homologues that Vary in Ring Size

Annemiek D. Knijnenburg,^[a] Adriaan W. Tuin,^[a] Emile Spalburg,^[b]
 Albert J. de Neeling,^[b] Roos H. Mars-Groenendijk,^[c] Daan Noort,^[c] José M. Otero,^[d, e]
 Antonio L. Llamas-Saiz,^[f] Mark J. van Raaij,^[d, g] Gijs A. van der Marel,^[a]
 Herman S. Overkleeft,^[a] and Mark Overhand*^[a]

Abstract: Monobenzylated sugar amino acids (SAAs) that differ in ether ring size (containing an oxetane, furanoid, and pyranoid ring) were synthesized and incorporated in one of the β -turn regions of the *cyclo*-decapeptide gramicidin S (GS). CD, NMR spectroscopy, modeling, and X-ray diffraction reveal that the ring size of the incorpo-

rated SAA moieties determines the spatial positioning of their *cis*-oriented carboxyl and aminomethyl substituents, thereby subtly influencing the amide

Keywords: amino acids • antimicrobial peptides • conformation analysis • gramicidin S • β -turn

linkages with the adjacent amino acids in the sequence. Unlike GS itself, the conformational behavior of the SAA-containing peptides is solvent dependent. The derivative containing the pyranoid SAA is slightly less hydrophobic and displays a diminished haemolytic activity, but has similar antimicrobial properties as GS.

Introduction

Sugar amino acids (SAAs) have found wide attraction in bioorganic chemistry research in the past decades.^[1] SAAs are broadly defined as carbohydrate-derived structures featuring both an amine and a carboxylate. They can be viewed as carbohydrate mimics or as amino acid mimics and as such are used in the design of oligomeric structures resembling oligosaccharides or oligopeptides, respectively.^[2] The sugar ring of SAAs can confer conformational rigidity onto an oligomer,^[3] and additional conformational constraints can be introduced by making use of bicyclic SAA building blocks, whereas linear SAAs can be used to achieve the opposite.^[4] The number and positioning of functional groups inherent to the parent monosaccharides give rise to a wealth of distinct SAA building blocks, in which specific features can be introduced by derivatization.^[5] SAAs mimicking α - or β -amino acids are available next to SAAs in which the amine and carboxylate are positioned more distal, providing γ - or δ -amino acids, giving rise to dipeptide isosteres.^[6]

Over the past few years we have focused on the study of gramicidin S (GS) analogues featuring SAA dipeptide isosteres in one or both turn regions.^[7] GS is a C₂-symmetric *cyclo*-decapeptide ((Pro-Val-Orn-Leu-D-Phe)₂) produced by the soil bacterium *Aneurinibacillus migulanus* (formerly *Bacillus brevis*)^[8,9] and consists of two β -strands interconnected by two type II' β -turns (**1** in Scheme 1). The two β -strands contain hydrophilic (Orn) and hydrophobic (Val and Leu) amino acids, and the type II' β -turns contain D-Phe-Pro sequences. Four intramolecular hydrogen bonds stabilize the antiparallel β -sheet with the hydrophilic and hydrophobic

[a] A. D. Knijnenburg, Dr. A. W. Tuin, Prof. Dr. G. A. van der Marel, Prof. Dr. H. S. Overkleeft, Dr. M. Overhand
 Leiden Institute of Chemistry
 Leiden University, P.O. Box 9502
 2300 RA Leiden (The Netherlands)
 Fax: (+31) 715274307
 E-mail: overhand@chem.leidenuniv.nl

[b] E. Spalburg, Dr. A. J. de Neeling
 National Institute of Public Health and the Environment
 Laboratory for Infectious Diseases
 P.O. Box 1, 3720 BA Bilthoven (The Netherlands)

[c] R. H. Mars-Groenendijk, Dr. D. Noort
 TNO, Prins Maurits Laboratory
 P.O. Box 45, 2280 AA Rijswijk (The Netherlands)

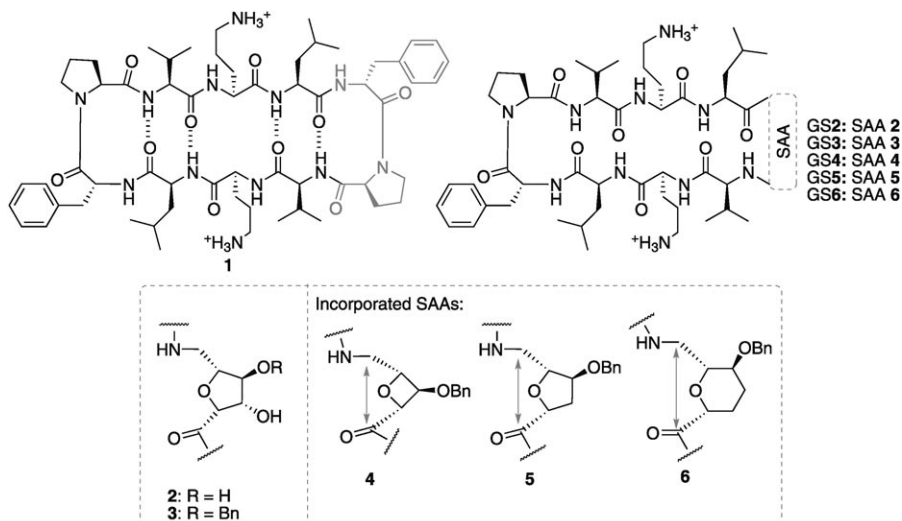
[d] Dr. J. M. Otero, Dr. M. J. van Raaij
 Departamento de Bioquímica y Biología Molecular
 Facultad de Farmacia, Edificio CACTUS
 Campus Sur, Universidad de Santiago
 15782 Santiago de Compostela (Spain)

[e] Dr. J. M. Otero
 Laboratoire des Proteines Membranaires
 Institut de Biologie Structurale J. P. Ebel
 41 Rue Jules Horowitz, 38027 Grenoble (France)

[f] Dr. A. L. Llamas-Saiz
 Unidad de Rayos X (RIAIDT), Laboratorio Integral
 de Dinámica y Estructura de Biomoléculas "José R. Carracedo"
 Edificio CACTUS, Campus Sur, Universidad de Santiago
 15782 Santiago de Compostela (Spain)

[g] Dr. M. J. van Raaij
 Departamento de Estructura de Macromoléculas
 Centro Nacional de Biotecnología, Campus Cantoblanco
 c/Darwin 3, 28049 Madrid (Spain)

Supporting information for this article is available on the WWW under <http://dx.doi.org/10.1002/chem.201002895>.



Scheme 1. GS (**1**) and GS analogues **2–6** with a sugar amino acid modified turn region containing a monobenzyloxy oxetane- (**4**), furanoid- (**2, 3**, and **5**), or pyranoid (**6**) ring. The arrows indicate the increasing distance between the carboxyl and aminomethyl substituents.

side chains positioned on opposing faces, thereby creating an amphiphatic structure.^[10] GS is an effective bactericidal agent against several Gram-positive and -negative bacteria.^[11] However it also lyses human red blood cells and is, therefore, only used as an antibiotic to treat topical infections.^[12]

In our previous studies, we found that replacing one of the D-Phe-Pro sequences with furanoid SAA **2** (Scheme 1) led to a GS analogue (GS2) featuring a β -strand structure highly reminiscent to that of the parent compound itself. Interestingly, X-ray diffraction studies of this compound, GS2, revealed that six GS2 monomers assemble in a β -barrel-like structure in a fashion that invited speculation on the mode of action by which GS (derivatives) penetrate cell membranes.^[13a] However, GS2 displayed minimal biological activity. In a subsequent study we capitalized on the presence of the hydroxyl groups in SAA **2** to introduce an additional functionality. By simply replacing SAA **2** by its monobenzylated counterpart **3** a more hydrophobic GS analogue (GS3) was obtained with structural and conformational features closely related to GS and GS2, but with biological activities largely restored (both bactericidal activity against an array of bacterial strains, as well as haemolytic activity).^[13b]

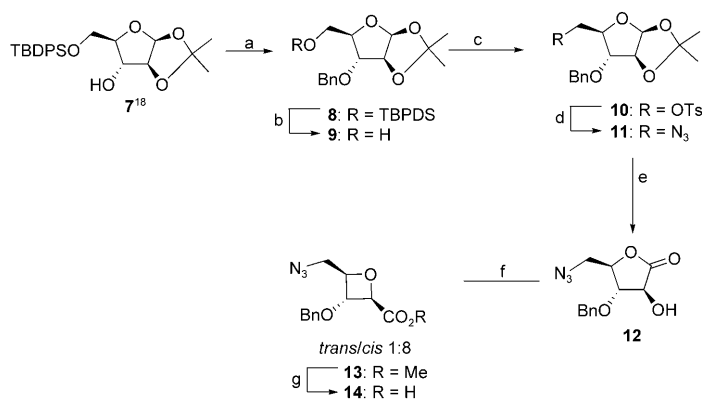
Subtle structural alteration of the incorporated SAA while leaving other features intact can thus have a major impact on the biological properties of a cyclic peptide.^[14] Encouraged by this observation we here set out to study the influence of ring-size of the incorporated SAA building block on the structure and activity of GS analogues. Going from a four-membered ether ring (oxetane SAA **4**) through a five-membered ether ring (furanoid, SAA **5**)^[15] to a six-membered ether ring (pyranoid, SAA **6**), while leaving all other features intact, leads to a gradual increase in the distance between the *cis*-oriented carboxyl and the aminomethyl substituents of the SAA in the β -turn region.^[16] We were

curious to find out what effect this has on the overall structural integrity and biological activity of GS analogues thus designed. Here we present the synthesis of the monobenzyloxy oxetane- and pyranoid building blocks **14** and **22**, their use in a solid-phase peptide synthesis approach and the structural and biological evaluation of the peptides GS4–6.

Results and Discussion

Synthesis: In the first instance, we turned our attention to the construction of the three suitably protected SAA building blocks **4–6**. Furanoid SAA **5** was prepared as its azide derivative by following a previously reported procedure.^[15] To get access to the azide of SAA **4** and **6**, we developed new procedures as outlined below.

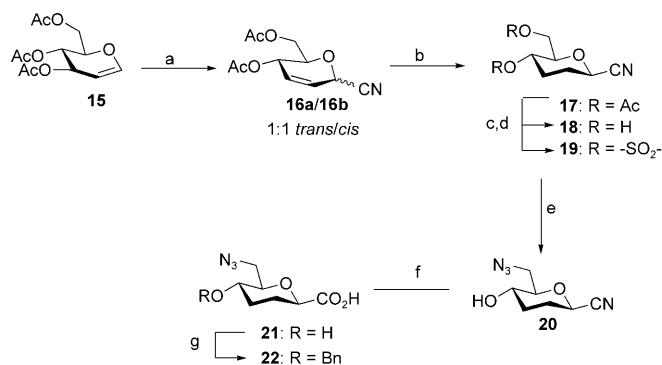
Oxetane SAAs can be obtained through a ring contraction of an α -triflyloxy γ -lactone^[17] and our synthesis towards the benzylated SAA **4** is based on this approach. Benzylation of the C-3 hydroxyl of the known protected D-arabinose **7** (Scheme 2)^[18] gave compound **8**. Desilylation, tosylation, and subsequent substitution with sodium azide gave compound **11** in 74% yield over three steps. The isopropylidene protective group was removed and oxidation of the intermediate anomeric acetal with bromine provided γ -lactone **12**. Triflation of γ -lactone **12** and ring contraction in basic methanol yielded 2,4-*cis*-oxetane **13** in 37% yield as a 1:8 *trans/cis* mixture of isomers. Hydrolysis of the *cis*-methyl



Scheme 2. a) BnBr, NaH, DMF, 0°C, 71%; b) TBAF in THF, 99%; c) TsCl, pyridine, 60°C, 87%; d) NaN₃, DMF, 95°C, 86%; e) 1) 70% AcOH, 2) Br₂, H₂O, 82% over 2 steps; f) 1) Tf₂O; 2) MeOH, K₂CO₃, 37% over 2 steps; g) NaOH, H₂O, 96%. TBAF = tetrabutylammonium fluoride.

ester **13** produced the desired 2,4-*cis*-oxetane **14** in an overall yield of 15% (over seven steps).

The 2,6-*cis*-pyranoid SAA **22** was synthesized by modification of a reported route.^[19] By starting from known tri-*O*-acetyl-D-glucal (**15**; Scheme 3), the cyanide functionality was introduced at the anomeric position through a Ferrier rear-



Scheme 3. a) $\text{BF}_3 \cdot \text{OEt}_2$, TMSCN, CH_2Cl_2 , **16a** (*trans*): 52%, **16b** (*cis*): 41%; b) 10% Pd/C, 0.02 M EtOH, 79%; c) DOWEX H^+ , MeOH, 60 °C, 88%; d) 1) SOCl_2 , pyridine, EtOAc, 2) RuCl_3 , NaIO_4 , $\text{H}_2\text{O}/\text{ACN}/\text{CH}_2\text{Cl}_2$, 93%; e) 1) NaN_3 , DMF, 80 °C, 2) H_2SO_4 in MeOH/THF, 95%; f) HCl, 100 °C, 86%; g) BnBr, 2 equiv NaH, DMF, 38%.

angement to give compounds **16a** and **16b** as a mixture of *trans/cis* anomers that could be separated by using silica gel chromatography. The double bond in the *cis*-compound **16b** was reduced, followed by deacetylation and introduction of a sulfonyl group to provide compound **19** in 65% yield over the three steps.^[20] Cyclic sulphate **19** was treated with sodium azide and subsequently with acid to give compound **20**.^[21] Intermediate **20** was hydrolyzed to provide carboxylic acid **21**. Finally a benzyl group was introduced at the C-4 hydroxyl functionality to give 2,6-*cis*-pyranoid SAA **22** (20% overall yield by starting from **16b**, Scheme 3).

Previously we reported^[15] the synthesis of 3-benzyloxy-2,5-*cis*-furanoid azido acid and the use of this building block in the synthesis of GS5. By following a similar protocol, the sugar azido acids **14** and **22** were used to obtain the cyclic peptides GS4 and GS6 (Scheme 1). This procedure involved the use of highly acid-sensitive HMPB-BHA resin to give two fully protected immobilized linear oligomers,^[7a,15] mild acidic cleavage from the solid support, and cyclization under high dilution with a coupling reagent cocktail of benzotriazol-1-yl-oxytripyridinophosphonium hexafluorophosphate (PyBOP), 1-hydroxybenzotriazole (HOBt), and *N,N*-diisopropylethylamine (DIPEA). After complete deprotection with strong acid (trifluoroacetic acid (TFA)) the peptides GS4 and GS6 were purified by preparative HPLC in 21 and 33% overall yields, respectively.

NMR spectroscopic analysis: The peptides GS4–6 show well dispersed 1D ^1H NMR spectra in water ($\text{H}_2\text{O}/\text{D}_2\text{O}$ 16:1) and methanol (CD_3OH), respectively. 2D NMR spectra (COSY, TOCSY, and cROESY^[22]) recorded in both solvent systems were used to fully assign the amino acid residues. ^1H homonuclear techniques^[23] were applied to obtain additional information concerning the local environment of an amino acid residue in the cyclic sequences. Excluding the SAA moieties, the $^3J_{\text{HN}\alpha}$ coupling constants of analogues GS4–6 resemble the typical GS cyclic β -hairpin structure with two strand regions (7–9 Hz for Val, Orn, and Leu residues) and a turn region (4 Hz for D-Phe; Figure 1A).^[23,24] This characteristic hairpin motif is also observed from the chemical shift perturbation values of GS4–6 (Figure 1B), which indicates that the Val, Orn, and Leu residues ($\Delta\delta_{\text{H}\alpha} > 0.1$ ppm) are part of a β -strand and the Pro and D-Phe residues ($\Delta\delta_{\text{H}\alpha} < 0$ ppm) are part of a β -turn.^[25] Generally lower coupling constant values and chemical shift perturbations of GS4–6 are observed in water when compared to the obtained data with methanol as the solvent (Figure 1A and B).^[26]

The amide proton exchange rates were measured by temperature coefficient experiments (Figure 1C) and the high exchange rates of the amide protons of the Orn and D-Phe residues indicate that these are solvent exposed and thus not involved in hydrogen-bonding interactions.^[27] Both the Val and Leu residues (with the exception of Leu4 in GS4) are not solvent exposed, which indicates their involvement in intramolecular hydrogen bonding. Comparison of the temperature coefficients measurement for peptides GS4–6 with those of GS indicates a similar intramolecular hydrogen-bonding pattern. A gradual increase in solvent exposure of the amide proton of the SAA moieties is found in the series oxetane, furanoid, and pyranoid SAA (Figure 1C).

The well-resolved 2D cROESY spectra revealed numerous sequential and long-range cross-peaks (Table 1, see also the Supporting Information). The absence of $\text{H}_\alpha^i/\text{H}_\alpha^{i+1}$ cross-peaks and the presence of $\text{H}_\alpha^i/\text{H}_\alpha^{i+1}$ cross-peaks (with the exception of the Pro residue) confirmed that all the amide bonds are in the *trans* conformation.^[23] The NOE signals observed in the SAA-modified β -turn are depicted in Figure 2. In all three cyclic peptides a long-range NOE between the amide protons of Val2 and Leu9 is observed (Figure 2A–C, arrow a), which indicates a hydrogen-bonding in-

Table 1. Cytotoxic (haemolytic) and antimicrobial activity (MIC, mgL^{-1}) of GS and GS analogues.

Analogue	Retention times ^[a] [min]	Erythrocytes ^[b]	<i>S. aureus</i> ^[c]	<i>S. epidermidis</i> ^[c]	<i>E. faecalis</i> ^[c]	<i>B. cereus</i> ^[c]	<i>P. aeruginosa</i> ^[d]	<i>E. coli</i> ^[d]
GS	8.38	31.2	8	8	8	8	64	32
GS4	6.21	> 500	32	16	64	16	> 64	64
GS5	6.96	125	16	16	32	16	> 64	64
GS6	7.22	500	16	8	16	8	> 64	32

[a] Retention times from RP-HPLC in minutes (see the Experimental Section). [b] Peptide concentration required for 100% lysis of erythrocytes in μM . The peptides were tested in triplicate. [c] Gram-positive bacteria, MIC (MIC = minimal inhibitory concentration) in mgL^{-1} . [d] Gram-negative bacteria, MIC mgL^{-1} MW including $2 \times \text{TFA}$ anion GS: 1369.49; GS3: 1344.44; GS4: 1358.47; GS5: 1372.49. MIC values were determined after 24 h of incubation with an experimental error of one MIC interval (a factor two, see the Experimental Section).

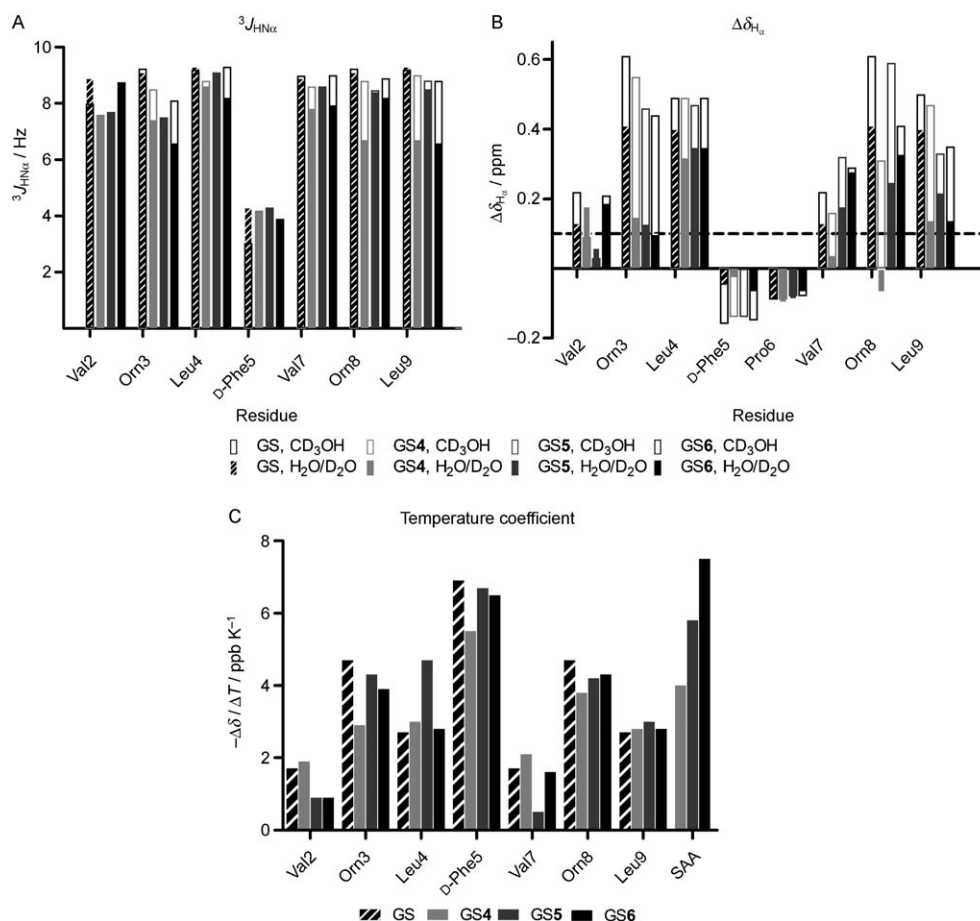


Figure 1. A) $^3J_{\text{HNHa}}$ (Hz) in H_2O (6% D_2O) and CD_3OH at 298 K. B) $\Delta\delta_{\text{Ha}}$ ($=\delta_{\text{Ha}}$ observed $-\delta_{\text{Ha}}$ random coil) in H_2O and CD_3OH at 298 K. C) Temperature coefficient reported as $-\Delta\delta/\Delta T$ in ppb/K measured in DMSO. Numbering of amino acids: *cyclo*-(SAA1-Val2-Orn3-Leu4-d-Phe5-Pro6-Val7-Orn8-Leu9).

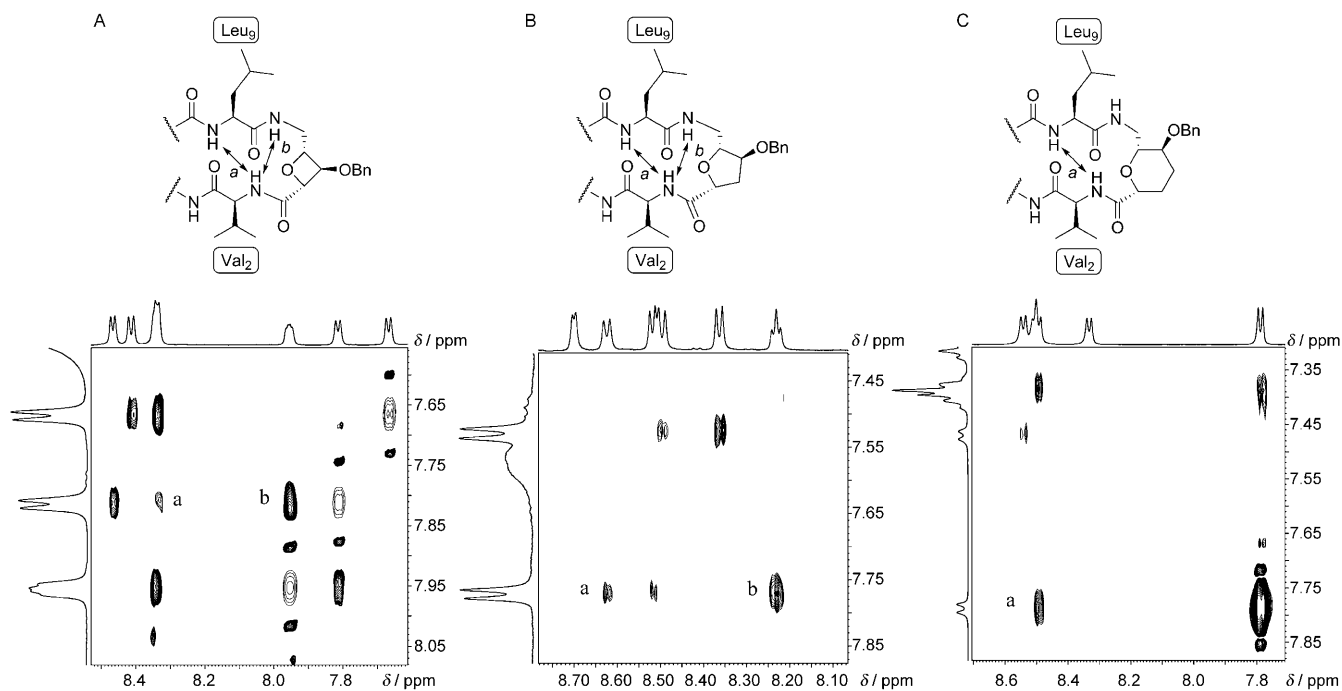


Figure 2. NH/NH cross-peak area of GS4 (A), GS5 (B), and GS6 (C). Arrows indicate the long-range cross-peaks. Spectra were recorded in $\text{H}_2\text{O}/\text{D}_2\text{O}$ 16:1.

teraction between the carbonyl of Val2 and the amide proton of Leu9.^[23] This is corroborated by the temperature coefficient experiments shown in Figure 1C. A NOE signal is observed between the protons of the SAA amide of GS4 and GS5 with the amide of the Val2 residue (Figure 2A and B, arrow b), which indicates that the incorporated oxetane and furanoid SAAs slightly alter the positioning of the amide linkage with Leu9. Importantly in GS6 this NOE signal is not observed.

Circular dichroism: The typical β-sheet/β-turn structure of all analogues is corroborated by measuring the CD spectra of GS and GS4–6 at 0.1 mM in water and in methanol (Figure 3). Two negative minima around 205 and 222 nm are visible which confirms the β-sheet and β-turn present in the secondary structure.^[28] GS adopts the same secondary struc-

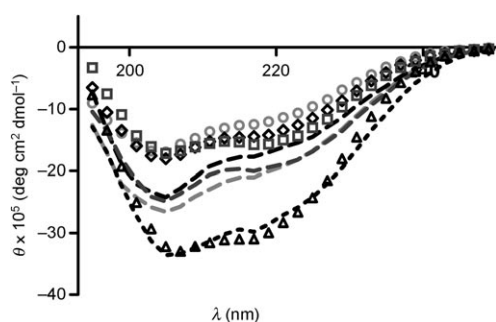


Figure 3. CD spectra at 0.1 mM in water (0.01 M NaOAc, pH 5.3) and at 0.1 mM in methanol of GS and analogues GS4–6. ○: GS4, H₂O; ---: GS4, CH₃OH; ◇: GS5, H₂O; ----: GS5, CH₃OH; □: GS6, H₂O; - - - -: GS6, CH₃OH; △: GS, H₂O; - · - · - ·: GS, CH₃OH.

ture in water and in methanol. However analogues GS4–6 exhibit an enhancement in excitation, changing from water to methanol as the solvent, indicating a more pronounced secondary structure in methanol.

Computational structure determination: The NMR spectroscopic data of GS4–6 were used as restraints to generate computational models of the cyclic peptides (see Tables S2 and S3 in the Supporting Information, Figure 4). Sequential and long-range NOE cross-peaks were quantified by using the isolated spin-pair approximation.^[29] For additional dihedral angles and hydrogen-bond constraints, respectively, amide coupling constants, chemical shift perturbations, and amide exchange values were used.^[30] The previously reported^[13a] X-ray structure of GS2 was used as the backbone starting structure in a distant geometry (DG) calculation. DG calculations with a modified^[31] version of the program DISGEO^[32] were used to generate an assembly of structures. The five structures with the smallest total error (violation < 0.1 Å, see Table S3 in the Supporting Information) were further refined by using the CVFF force field^[33] (Biosym) and an average structure was generated (Figure 4A–C). The generated structures of GS4–6 all exhibit a twisted structure (twisting angle $\theta = 20\text{--}45^\circ$), which is common for these types of cyclic peptides.^[34] The oxetane SAA in the β-turn (GS4) induces the highest sheet twisting (twisting angle θ at around $\sim 45^\circ$).^[35] In the calculated structures of GS4 and GS5 the amide linkage between Leu9 and the SAA moieties is reoriented: the ψ angle of Leu9 as indicated in Figure 4D and E is between $90\text{--}100^\circ$. The corresponding ψ dihedral angle of Leu9 in GS6 is $\sim 130^\circ$ and

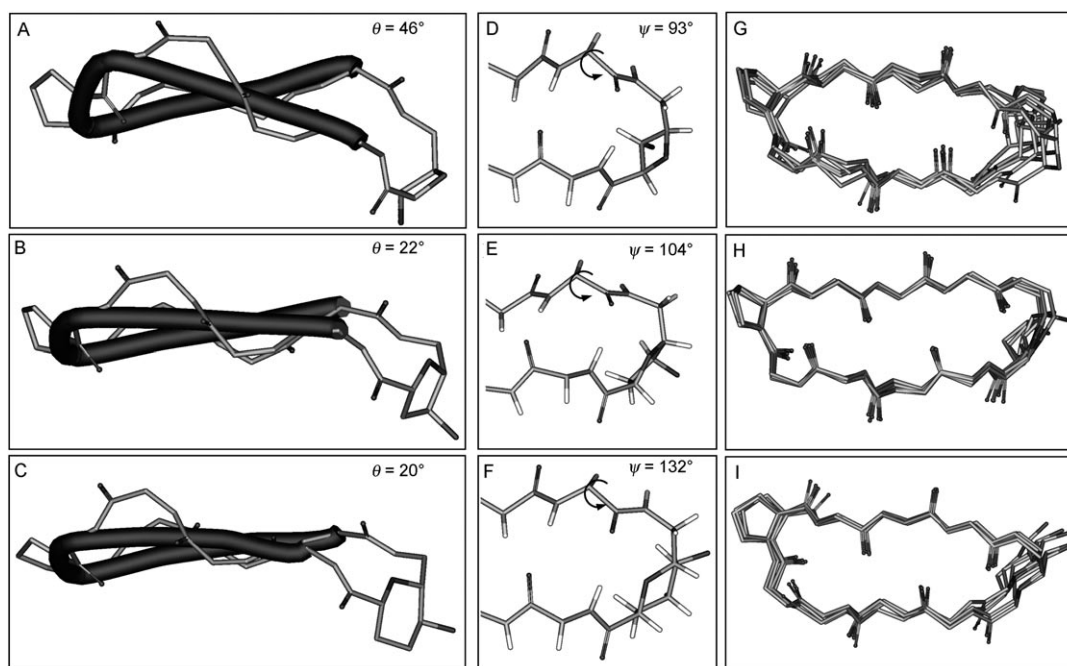


Figure 4. A)–C) Side view of average DG structures of GS4–6, side chains are omitted for clarity. D)–F) Top view of average structures of GS4–6. G)–I) Superimposed structures of GS4–6 (r.m.s.d. GS4: 0.37 ± 0.05 ; GS5: 0.23 ± 0.06 ; GS6: 0.27 ± 0.04).

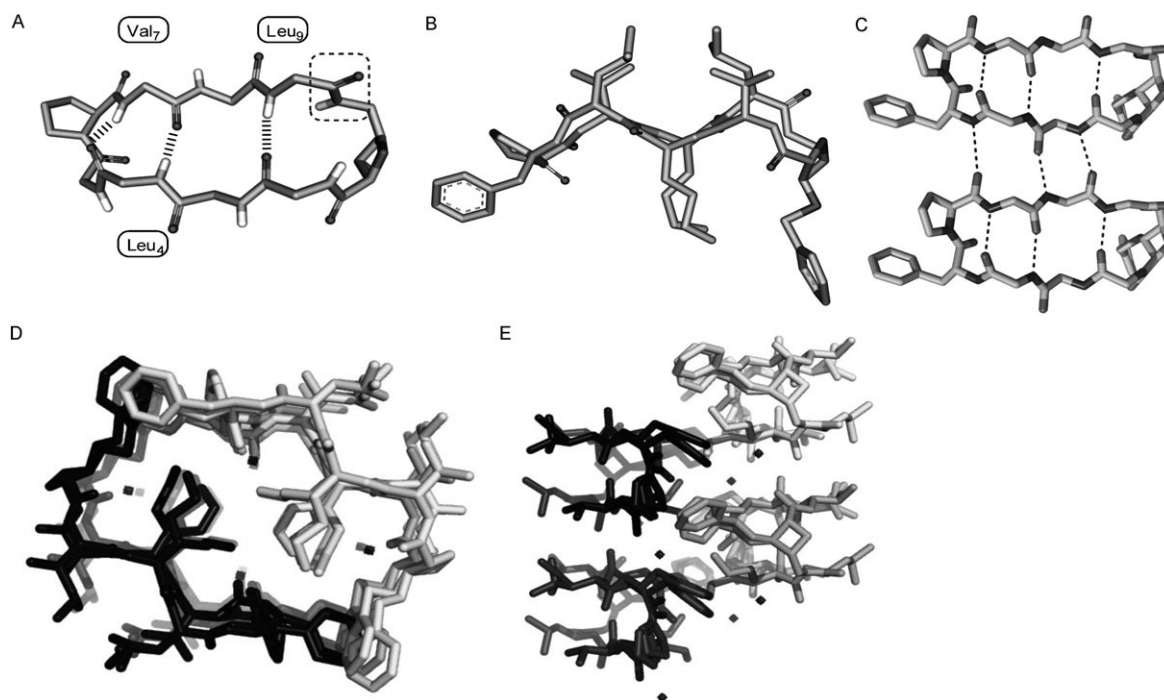


Figure 5. A) Top view of the X-ray structure of GS4, $\psi = 13.5^\circ$, side chains are omitted for clarity. Intramolecular hydrogen bonds are indicated by dashed lines. B) Side view of the crystal structure of GS4. C) Intermolecular and intramolecular hydrogen bridges observed in the crystal lattice. D) Top view of the crystal packing along the a axis. E) Side view of the crystal packing along the c axis.

more closely resembles a regular β -strand dihedral ψ angle ($\sim 120^\circ$).^[23]

X-ray analysis: High-quality crystals of GS4 were grown from a methanol/water mixture. The crystal structure was resolved and refined to 1.0 Å resolution (the diffraction limit of the crystals, see Table S1 in the Supporting Information). The crystal structure of GS4 confirms the overall β -sheet/ β -turn structure. In total, three hydrogen bridges are observed, involving the amides of Leu4, Val7, and Leu9 (Figure 5A). Some differences with the computational structure were observed. The X-ray structure exhibited a less twisted pleated-sheet structure ($\theta = 18^\circ$, Figure 5B) and the amide reorientation is more pronounced (Leu9 $\psi = 13.5^\circ$; Figure 5A indicated in the dashed box). The crystallographic analysis of GS4 revealed a shorter β -sheet shape than native GS, with three intramolecular hydrogen bonds and parallel disposition of the β -sheets forming infinite “cylindrical” structures with all the hydrophobic residues in the surface and the hydrophilic residues pointing to the centre (Figure 5C–E). The size of the pore in this aggregate is smaller than in native GS.^[34]

Physical and biological properties: Cyclic peptides GS4–6 were screened for their antimicrobial activity against several Gram-positive and -negative strains (Table 1). GS6 exhibits comparable activity to native GS towards the screened micro-organisms. GS5 displays marginally less activity and GS4 shows a substantially decreased antimicrobial activity. All the compounds were also evaluated on their activity in

lysing erythrocytes (Table 1, Figure 6). Interestingly, GS5 and GS6 show a four- and 15-fold decrease in haemolytic activity, respectively, as judged by the determined concentrations required for 100% haemolysis (Table 1). GS4 exhibits the least haemolytic activity with a 100-fold decrease in haemolytic activity relative to GS.

In previous studies^[36] with related antimicrobial peptides, it was found that an optimum an optimal hydrophobicity (as monitored by their retention times) was observed with respect to their biological profile. It was found that compounds that are slightly less hydrophobic than GS are also less toxic, while retaining potent antimicrobial activity.^[36a] Therefore, determination of retention time under controlled conditions on RP-HPLC was used as a measure of the pep-

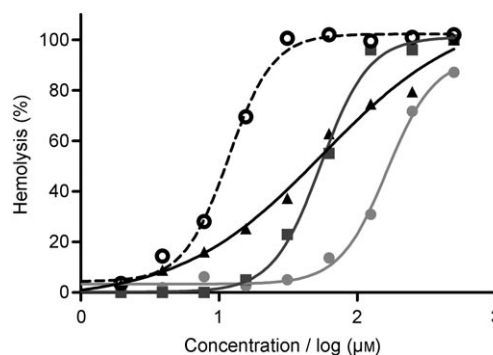


Figure 6. Haemolytic activity of analogues GS4–6 and GS. Experiments were carried out in duplicate with a maximum of 10% experimental error. ●: GS4; ■: GS5; ▲: GS6; ○: GS.

tide hydrophobicity. GS4 is the least hydrophobic in this series of compounds, whereas GS6 is slightly less hydrophobic than GS, on the basis of their retention times (Table 1).

Conclusion

In this report we present a study to evaluate the effect of ring size of SAAs as type II' β -turn mimics on the structural and biological properties of GS-derived cyclic peptides. Homologues GS4–6, containing a monobenzylated oxetane, furanoid, and pyranoid SAA, respectively, exhibit well-defined cyclic hairpin structures in solution. However, as the structures of the peptides GS4–6 show solvent dependence, they are not as rigid as GS. Sugar amino acid dipeptide isosteres are generally considered more rigid than the corresponding dipeptide moieties they replace.^[1,6] In cyclic peptides, as is shown here, this may not always be the case because of the strict geometrical requirements of the secondary structure.^[30d]

As anticipated the distance between the *cis*-oriented carboxyl and the aminomethyl substituents of the ether rings becomes larger going from a four-membered (oxetane SAA 4) through a five-membered (furanoid, SAA 5) to a six-membered ether ring (pyranoid, SAA 6; Figure 7A). The

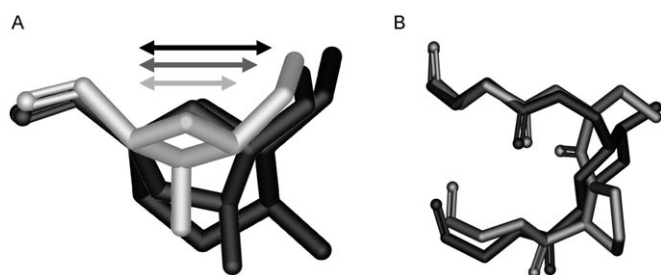


Figure 7. A) Overlay of the different ring-size sugar amino acids (4–6) incorporated in gramicidin S, oxetane in light grey, furanoid in dark grey and pyranoid in black. B) Overlay of SAA 6 (black) with the X-ray structure of the D-Phe-Pro sequence of GS (grey).

overall effect of the difference in ring size is that the amide linkage between the adjacent leucine residue with the SAA moiety is subtly reoriented in the oxetane (GS4) and furanoid case (GS5) leaving the rest of the hairpin structure largely intact, whereas the pyranoid (of GS6) is the best mimic of the D-Phe-Pro two-residue turn motif (Figure 7B). The difference in the calculated structure of GS4 and its X-ray structure is attributed to packing in the crystal. From a biological point of view, SAA6 can be viewed as an improved version of the D-Phe-Pro sequence of GS. The antimicrobial activity of GS6 (containing SAA 6) is similar to that of GS and markedly better than GS5 and GS4. Of interest is that GS6 displays a significantly decreased haemolytic activity relative to GS. As GS6 is slightly less hydrophobic than GS (as empirically determined by their retention times (Table 1)), it follows the general trend observed with related

antimicrobial peptides:^[36] that compounds that are slightly less hydrophobic than GS are also less toxic while retaining antimicrobial activity.^[36a] It should be noted that this general trend is followed at low peptide concentration, but that at higher peptide concentration the less hydrophobic GS5 is more haemolytic than GS6 (see Figure 6). A possible explanation for this observation might be the subtle changes in secondary structure.

The relation of antimicrobial activity and haemolytic activity is complex due to the diversity in membrane structures of microorganisms. Several models^[37] have been proposed for the membrane disruption mechanism of GS and it would be of interest to investigate whether the conformationally changed peptides (GS4–6) exhibit the same membrane disrupting characteristics. Despite the exhaustive conformational analysis as described here we do not fully comprehend the correlation between the flexibility and biological activity of the peptides. Whether the conformational flexibility of the modified peptides GS4–6 can be used for the future design of compounds with enhanced biological properties remains subject for further research.

In summary, we have identified a GS derivative (GS6) with reduced haemolytic activity and largely retained the antimicrobial activity. Thus, the strategy to design and synthesize a series of homologues with decreasing hydrophobicity and subtle conformational changes presented here proves to be fruitful to obtain a compound with improved properties. Currently, we are investigating the haemolytic properties of GS6 exceeds its slightly decreased antimicrobial activity in more advanced biological assays and animal infection models.

Experimental Section

General: Light petroleum ether (Petet) with a boiling range of 40–60 °C was used. All other solvents used under anhydrous conditions were stored over 4 Å molecular sieves except for methanol, which was stored over 3 Å molecular sieves. Solvents used for workup and column chromatography were of technical grade and distilled before use. All other solvents were used without further purification. Reactions were monitored by TLC analysis. Elemental analyses were carried out with a Perkin-Elmer Series II CHNS/O analyzer 2400. The linear peptides were cleaved from resin, cyclized, and purified by RP-HPLC (Gilson GX-281) with a preparative Gemini C18 column (Phenomenex 150 × 21.2 mm, 5 μ m particle size). The applied eluents were A: 0.1% aq. TFA, B: MeCN. The linear peptides and cyclized peptides were analyzed with LCMS (detection simultaneously at 214 and 254 nm) equipped with an analytical C18 column (4.6 mmD × 250 mmL, 5 μ m particle size). The applied buffers were A: H₂O, B: MeCN, and C: 1.0% aq. TFA. HRMS were recorded by direct injection (2 μ L of a 2 μ M solution in H₂O/MeCN 50:50 *v/v* and 0.1% formic acid) on a mass spectrometer Thermo Finnigan LTQ Orbitrap equipped with an electrospray ion source in positive mode (source voltage 3.5 kV, sheath gas flow 10, capillary temperature 523 K) with resolution $R=60000$ at $m/z: 400$ (mass range $m/z: 150-2000$) and diethylphthalate ($m/z: 391.28428$) as lock mass. Optical rotations were measured on a Propol automatic polarimeter (sodium D-line, $\lambda=589$ nm). Specific rotations $[\alpha]_D$ are given in degree per centimeter and the concentration c is given in mg mL^{-1} in the specific solvent. IR spectra were recorded on a Perkin-Elmer Paragon 1000 FTIR spectrometer.

NMR spectroscopy: ^1H and ^{13}C NMR spectra for all intermediates (7–22) were recorded on a Bruker AV-400 (400/100 MHz). The spectra of the peptides (GS4–6) were recorded on a Bruker DMX 600 equipped with a pulsed field gradient accessory and a cryo-probe. For the 2D cROESY spectra (200 msec mixing time) the peptides were dissolved 7 mg mL^{-1} in a 6% $\text{D}_2\text{O}/\text{H}_2\text{O}$ mixture. Standard DGF-COSY ($512\text{c}\times 2084\text{c}$) and TOCSY ($400\text{c}\times 2048\text{c}$) spectra were recorded by using presaturation for solvent suppression. cROESY^[22] spectra ($400\text{c}\times 2048\text{c}$, $\tau_{\text{mix}}=180\text{ ms}$) were recorded by using the presat solvent suppression. All spectra were recorded in phase-sensitive mode, by using either the TPPI or states-TPPI for quadrature detection in the indirect dimension. Homonuclear coupling constants were determined from the corresponding ^1H spectra.

Structure generation: The computational structure determinations were performed on a Silicon Graphics O2 by using the program Insight-II. Distant geometry (DG) calculations were carried out with the DISCOVER program by using the CVFF force field^[33] and a dielectric constant of 1. A modified^[31] version of the program DISGEO^[32] in combination with interproton distances, dihedral angles (ϕ out of $^3J_{\text{NH}\alpha}$ and using the Karplus^[30a] equation; ψ out of $\Delta\delta_{\text{H}\alpha}$ to a distance of 1.78 \AA . Regions on both sides of the diagonal were analyzed. Pseudoatom corrections were taken into account. The upper and lower bond restraints were set as distance $\pm 10\%$, accounting for the experimental error. The DG calculation was performed by using the X-ray structure of compound GS2 (TM5025)^[13a] as the starting structure.

CD spectroscopy: CD spectra were recorded at 298 K on a Jasco J-815 spectropolarimeter by using 0.1 cm path length quartz cells. The CD spectra are averages of four scans, collected at 0.1 nm intervals between 190 and 250 nm with a scanning speed of 50 nm min^{-1} . The peptides were prepared at concentrations of 0.1 mM in CH_3OH and H_2O (0.01 M NaOAc, pH 5.3). Ellipticity is reported as mean residue ellipticity $[\theta]$, with approximate errors of $\pm 10\%$ at 220 nm.

Crystallization and crystal structure determination of compound GS4: Colorless needle-shaped crystals were obtained after slow evaporation of droplets (2 μL) of GS4 (10 mg mL^{-1}) in a 40% solution of MeOH in H_2O plus NaOH in MeOH (2 μL , 0.5 M) under paraffin oil in a Terasaki plate. A $0.5\times 0.01\times 0.01\text{ mm}$ crystal was mounted in air and then rapidly placed under liquid nitrogen. Screening of several crystals and preliminary diffraction tests were performed at beamline BM30A and high-resolution synchrotron data were collected at beamline ID23-2 at the ESRF (Grenoble, France). Images were collected by using DNA software,^[38] processed with XDS,^[39] and scaled with XPREP.^[39] The structure was solved by direct methods with the program SHELXD^[40] and refined with no intensity cutoff by using the full-matrix least-squares method on F^2 implemented in SHELXL^[40] and included in the WinGX package.^[41] Throughout the refinement, bond length, bond angle, planarity, and stereochemical restraints were imposed. All non-H atoms were refined anisotropically with suitable rigid bond and similarity restraints. All hydrogen positions were calculated and refined by using a riding atom model. There is a crystallographically independent molecule per asymmetric unit with several disordered amino acids. Selected crystallographic data is reported in Table S1 in the Supporting Information. Final figures were created by using PyMOL (Delano Scientific, Palo Alto CA, USA). CCDC-792843 contains the supplementary crystallographic data for this paper. These data can be obtained free of charge from The Cambridge Crystallographic Data Centre via www.ccdc.cam.ac.uk/data_request/cif.

Antibacterial assays: The following bacterial strains were used: *Staphylococcus aureus* (ATCC 29213), *Staphylococcus epidermidis* (ATCC 12228), *Enterococcus faecalis* (ATCC 29212), *Bacillus cereus* (ATCC 11778), *Escherichia coli* (ATCC 25922), and *Pseudomonas aeruginosa* (ATCC 27853). Bacteria were stored at -70°C and grown at 30°C on Columbia Agar with sheep blood (Oxoid, Wesel, Germany) suspended in physiological saline until an optical density of 0.1 AU (at 595 nm, 1 cm cuvette). The suspension was diluted ($10\times$) with physiological saline, and 2 μL of

this inoculum was added to 100 μL growth medium, Nutrient Broth from Difco (ref. nr. 234000, lot nr. 6194895) with yeastextract (Oxoid LP 0021, lot nr. 900711, 2 g/400 mL broth), in microtiter plates (96 wells). The peptides GS and GS4–6 were dissolved in ethanol (4 g L^{-1}) and diluted in distilled water (1000 mg L^{-1}), and two-fold diluted in the broth (64, 32, 16, 8, 4, and 1 mg L^{-1}). The plates were incubated at 30°C (24–96 h) and the MIC was determined as the lowest concentration inhibiting bacterial growth. The experiments were conducted once; the experimental error is one MIC interval (a factor two).

Haemolytic assays: Freshly drawn heparinized blood was centrifuged for 10 min at 1000 g at 10°C . Subsequently, the erythrocyte pellet was washed three times with 0.85% saline solution and diluted with saline to a 1/25 packed volume of red blood cells. The peptides to be evaluated (GS4–6 and GS) were dissolved in a 30% DMSO/0.5 mM saline solution to give a 1.5 mM solution of peptide. If a suspension was formed, the suspension was sonicated for a few seconds. A 1% Triton-X solution was prepared. Subsequently, 100 μL of saline solution was dispensed in columns 1–11 of a microtiter plate and 100 μL of 1% Triton solution was dispensed in column 12. To wells A1–C1, 100 μL of the peptide was added and mixed properly. 100 μL of wells A1–C1 was dispensed into wells A2–C2. This process was repeated until wells A10–C10, followed by discarding 100 μL of wells A10–C10. These steps were repeated for the other peptides. Subsequently, 50 μL of the red blood cell solution was added to the wells and the plates were incubated at 37°C for 4 h. After incubation, the plates were centrifuged at 1000 g at 10°C for 4 min. In a new microtitre plate, 50 μL of the supernatant of each well was dispensed into a corresponding well. The absorbance at 405 nm was measured and the percentage of hemolysis was determined. The experiment was conducted once and carried out in triplo. A maximum of 10% experimental error was found.

Synthesis: The general synthetic procedure of GS analogues and the intermediates towards SAA 14 and SAA 22 are reported in the Supporting Information.

2,4-Anhydro-5-azido-5-deoxy-3-O-benzyl-D-ribose acid (14): Compound 13 (0.71 mmol, 193 mg) was dissolved in $\text{THF}/\text{H}_2\text{O}$ (16 mL, 7:1) and 1 M of aq. NaOH was added (4 equiv 2.84 mL). The mixture was stirred for 16 h and TLC analysis showed full conversion into product ($R_f=0.19$, 1:1 EtOAc/Petet, 1% AcOH). The solvent was evaporated and the crude was ion-exchanged with Amberlite H^+ in H_2O to yield 14 as a colorless oil (0.68 mmol, 180 mg, 96%). $[\alpha]_{\text{D}}^{20} = +196.4$ ($c=0.5$ in CHCl_3); $^1\text{H NMR}$ (400 MHz, CDCl_3): $\delta=8.72$ (brs, 1H; OH), 7.41–7.28 (m, 5H; CH Ar), 5.06 (d, $J=5.2\text{ Hz}$, 1H; H_2), 4.76 (m, 1H; H_3), 4.73 (d, $J=12.0\text{ Hz}$, 1H; CH_2 Benzyl), 4.48 (d, $J=12.0\text{ Hz}$, 1H; CH_2 Benzyl), 4.51 (m, 1H; H_3), 3.36 ppm (ddd, $J=3.6, 13.9, 121.2\text{ Hz}$, 2H; H_5, H_6); $^{13}\text{C NMR}$ (101 MHz, CDCl_3): $\delta=173.8$ (C=O), 136.5 (C_q Ar), 128.6, 128.4, 128.1 (CH Ar), 84.8 (C_4), 81.4 (C_2), 76.3 (C_3), 72.1 (CH_2 Ar), 52.3 ppm (C_5); IR $\tilde{\nu}=2923.4$ (w), 2104.6 (s), 1735.5 (s), 1262.3 (s), 1126.7 cm^{-1} (s); HRMS (ESI): m/z : calcd for $\text{NaC}_{12}\text{H}_{13}\text{N}_3\text{O}_4$: 286.07983; found: 286.07986 $[\text{M}+\text{Na}]^+$.

6-Azido-4-O-benzyl-2,3-dideoxy- β -D-erythro-hexopyranosecarboxylic acid (22): Compound 21 (95 mg, 0.47 mmol) was co-evaporated with toluene ($3\times 50\text{ mL}$) and dissolved in DMF (30 mL). The solution was cooled to 0°C and 60% mineral oil NaH (2.5 equiv, 1.18 mmol, 47.2 mg) was added. After 20 min, benzyl bromide (1.1 equiv 0.52 mmol, 61 μL) was added and the reaction was stirred overnight. The reaction was quenched with H_2O and the volatiles were removed in vacuo. The residue was extracted with CH_2Cl_2 (20 mL) and 1 M HCl (100 mL). The aqueous layer was extracted three times with CH_2Cl_2 . The combined organic layers were dried with Na_2SO_4 and the volatiles evaporated. The residue was column purified (52 mg, 0.19 mmol, 38%, 1:5 EtOAc/Petet, 1% AcOH). $[\alpha]_{\text{D}}^{20} = +114.2$ ($c=1$, CHCl_3); $^1\text{H NMR}$ (400 MHz, CDCl_3): $\delta=^1\text{H NMR}$ (400 MHz, CDCl_3): $\delta=8.21$ (brs, 1H; COOH), 7.65–6.93 (m, 5H; CH Benzyl), 4.63 (d, $J=11.4\text{ Hz}$, 1H; CH_2 Benzyl), 4.44 (d, $J=11.4\text{ Hz}$, 1H; CH_2 Benzyl), 4.06 (d, $J=11.6\text{ Hz}$, 1H; H_1), 3.62 (d, $J=12.0\text{ Hz}$, 1H; $H_{6,6'}$), 3.48 (d, $J=12.8\text{ Hz}$, 2H; $H_{6,6'}$), 3.54–3.45 (m, 1H; H_5), 3.36 (m, 1H; H_4), 2.39 (m, 1H; H_3), 2.18 (d, $J=12.6\text{ Hz}$, 1H; H_2), 1.68 (qd, $J=13.6, 3.0\text{ Hz}$, 1H; H_2), 1.53 ppm (td, $J=13.4, 3.6\text{ Hz}$, 1H; H_5); $^{13}\text{C NMR}$ (101 MHz, CDCl_3): $\delta=173.94$ (COOH), 137.51 (C_q benzyl), 128.45, 127.94, 127.78 (CH benzyl), 79.79 (C_5), 75.27 (C_1), 72.77 (C_4), 70.86 (CH_2

benzyl), 51.47 (C_6), 28.46 (C_3), 27.54 ppm (C_2); IR = $\bar{\nu}$ = 2869.9, 2098.3, 1729.0, 1455.0, 1441.4, 1353.9, 1288.9, 1216.9, 1139.3, 1104.3, 739.5, 699.6, 629.1, 544.3 cm^{-1} ; HRMS (ESI): m/z : calcd for $\text{NaC}_{14}\text{H}_{17}\text{N}_3\text{O}_4$: 314.11113; found: 314.11126 [$M+\text{Na}$] $^+$.

cyclo-[SAA₄-Val-Orn-Leu-D-Phe-Pro-Val-Orn-Leu]-2 TFA (GS4): The cyclized deprotected peptide was RP-HPLC purified (linear gradient of 37–46%, 3 CV) and yielded 42.0 mg, 31.2 μmol , 21%. ^1H NMR (600 MHz, $\text{H}_2\text{O}+\text{D}_2\text{O}$): δ = 8.63 (d, J = 3.7 Hz, 1H; NH D-Phe₅), 8.47 (d, J = 7.3 Hz, 1H; NH Orn₃), 8.41 (d, J = 8.7 Hz, 1H; NH Leu₄), 8.34 (d, J = 6.8 Hz, 2H; NH Leu₉ Orn₈), 7.96 (dd, J = 3.7, 6.7 Hz, 1H; NH SAA₄), 7.81 (d, J = 7.6 Hz, 1H; NH Val₂), 7.67 (d, J = 7.8 Hz, 1H; NH Val₇), 7.54 (brs, 4H; NH₂ Orn), 7.41–7.17 (m, 10H; CH Ar), 5.00 (d, J = 5.4 Hz, 1H; H₂ SAA), 4.85 (m, 1H; H₄ SAA), 4.63 (m, 1H; H_α D-Phe₅), 4.78 (d, J = 11.2 Hz, 1H; CH₂ Benzyl), 4.30 (d, J = 11.2 Hz, 1H; CH₂ Benzyl), 4.50 (m, 2H; H_α Orn₃, Leu₄), 4.33 (m, 1H; H_α Pro₆), 4.30 (m, 2H; H_α Leu₉, Orn₈), 4.12 (t, J = 7.2 Hz, 1H; H_α Val₂), 4.09 (t, J = 5.4 Hz, 1H; H₃ SAA), 3.98 (t, J = 8.0 Hz, 1H; H_α Val₇), 3.61 (m, 1H; H_{βd} Pro₆), 3.54 (m, 1H; H_{sd} SAA₄), 3.23 (d, J = 15.5 Hz, 1H; H_{5u} SAA₄), 3.01 (m, 1H; H_{βdu} D-Phe₅), 2.92 (m, 2H; H_{βdu} Orn₃), 2.84 (m, 2H; H_{βdu} Orn₈), 2.75 (m, 1H; H_{3u} Pro₆), 2.09 (q, J = 7.0 Hz, 2H; H_β Val_{2,7}), 1.88 (m, 3H; H_{βdu} Pro₆, H_{βd} Orn₃), 1.81 (s, 1H; H_{βd} Orn₈), 1.74–1.50 (m, 8H; H_{βu,γdu} Orn, H_{γdu} Pro₆), 1.50–1.36 (m, 4H; H_{βdu} Leu), 1.32 (m, 2H; Hy Leu), 0.92 (d, J = 6.7 Hz, 3H; CH₃ Val₂), 0.89 (d, J = 6.7 Hz, 3H; CH₃ Val₂), 0.86 (d, J = 6.7 Hz, 3H; CH₃ Val₇), 0.83 (d, J = 6.9 Hz, 3H; CH₃ Val₇), 0.82 (d, J = 6.1 Hz, 3H; CH₃ Leu₉), 0.81 (d, J = 6.0 Hz, 3H; CH₃ Leu₉), 0.79 (d, J = 6.5 Hz, 3H; CH₃ Leu₄), 0.77 ppm (d, J = 6.4 Hz, 3H; CH₃ Leu₄); ^{13}C NMR (151 MHz, CD_3OH): δ = 175.01, 173.91, 173.71, 173.55, 173.45, 173.29, 172.89, 172.70, 138.76, 137.01, 130.50, 129.78, 129.59, 129.14, 128.87, 128.58, 86.50, 83.40, 77.84, 72.50, 62.12, 60.87, 60.40, 55.97, 53.96, 53.43, 52.90, 51.97, 49.58, 49.43, 49.29, 49.15, 49.01, 48.87, 48.72, 48.02, 42.33, 41.88, 40.89, 40.76, 37.48, 32.05, 31.75, 30.70, 30.42, 30.36, 25.90, 25.25, 24.83, 24.60, 23.89, 23.18, 23.14, 22.24, 19.88, 19.73, 19.39, 19.30 ppm; HRMS (ESI): m/z : calcd for $\text{C}_{58}\text{H}_{90}\text{N}_{11}\text{O}_{11}$: 1116.68158; found: 1116.68316 [$M+\text{H}$] $^+$; LCMS: R_t = 6.21 min, linear gradient 10 → 90% B in 13.5 min.; m/z : 1117.1 [$M+\text{H}$] $^+$.

cyclo-[SAA₅-Val-Orn-Leu-D-Phe-Pro-Val-Orn-Leu]-2 TFA (GS5): ^1H NMR (600 MHz, $\text{H}_2\text{O}+\text{D}_2\text{O}$): δ = 8.70 (d, J = 4.3 Hz, 1H; NH D-Phe₅), 8.63 (d, J = 8.5 Hz, 1H; NH Leu₉), 8.52 (d, J = 7.5 Hz, 1H; NH Orn₃), 8.50 (d, J = 9.1 Hz, 1H; NH Leu₄), 8.36 (d, J = 8.4 Hz, 1H; NH Orn₈), 8.23 (t, J = 6.1 Hz, 1H; NH SAA), 7.77 (d, J = 7.7 Hz, 1H; NH Val₂), 7.57 (brs, 4H; NH₂ Orn), 7.53 (d, J = 8.6 Hz, 1H; NH Val₇), 7.44–7.17 (m, 10H; CH Ar), 4.65–4.61 (m, 3H; H_α D-Phe₅, Orn₈, H₁ SAA), 4.55 (m, 2H; CH₂ Benzyl), 4.49 (m, 2H; H_α Orn₃, Leu₄), 4.40 (m, 1H; H_α Leu₉), 4.35 (dd, J = 2.9, 8.4 Hz, 1H; H_α Pro₆), 4.28 (s, 1H; H₄ SAA), 4.13 (t, J = 8.0 Hz, 1H; H_α Val₇), 4.09 (d, J = 5.3 Hz, 1H; H₃ SAA), 4.01 (t, J = 7.7 Hz, 1H; H_α Val₂), 3.62 (m, 1H; H_{βd} Pro₆), 3.58 (m, 1H; H_{5u} SAA), 3.25 (m, 1H; H_{5u} SAA), 3.04 (dd, J = 6.0, 12.9 Hz, 1H; H_{βd} D-Phe₅), 2.94 (m, 5H; H_{βu} D-Phe₅, H_{βdu} Orn), 2.67 (q, J = 8.3 Hz, 1H; H_{3u} Pro₆), 2.39 (dd, J = 6.2, 13.2 Hz, 1H; H_{sd} SAA), 2.09 (dq, J = 6.9, 13.9 Hz, 2H; H_β Val_{2,7}), 1.92–1.80 (m, 4H; H_{βd} Orn, H_{βdu} Pro₆), 1.73–1.29 (m, 14H; H_{βdu,γ} Leu, H_{βu,γdu} Orn, H_{γdu} Pro), 0.93, 0.91, 0.90, 0.88 (s, 12H; CH₃ Val_{2,7}), 0.82 (d, J = 6.1 Hz, 3H; CH₃ Leu₉), 0.81 (d, J = 5.9 Hz, 3H; CH₃ Leu₉), 0.79 (d, J = 6.4 Hz, 3H; CH₃ Leu₄), 0.78 ppm (d, J = 6.4 Hz, 3H; CH₃ Leu₄); HRMS (ESI): m/z : calcd for $\text{C}_{59}\text{H}_{92}\text{N}_{11}\text{O}_{11}$: 1130.69723; found: 1130.69918 [$M+\text{H}$] $^+$; LCMS: R_t = 6.96 min, linear gradient 10 → 90% B in 13.5 min.; m/z : 1131.0 [$M+\text{H}$] $^+$.

cyclo-[SAA₆-Val-Orn-Leu-D-Phe-Pro-Val-Orn-Leu]-2 TFA (GS6): The cyclized deprotected peptide was RP-HPLC purified (linear gradient of 38–42%, 3 CV) and yielded 45.8 mg, 33.4 μmol , 33%. ^1H NMR (600 MHz, $\text{H}_2\text{O}+\text{D}_2\text{O}$): δ = 8.76 (d, J = 3.5 Hz, 1H; NH D-Phe₅), 8.54 (d, J = 9.0 Hz, 1H; NH Leu₄), 8.51 (d, J = 7.1 Hz, 1H; NH Leu₉), 8.49 (d, J = 8.6 Hz, 1H; NH Orn₃), 8.33 (d, J = 8.6 Hz, 1H; NH Orn₈), 7.79 (d, J = 8.9 Hz, 1H; NH Val₂), 7.47 (d, J = 8.5 Hz, 1H; NH Val₇), 7.44–7.20 (m, 11H; CH Ar, NH SAA), 4.69 (m, 1H; H_α Orn₃), 4.64 (d, J = 11.1 Hz, 1H; CH₂ Benzyl), 4.59 (m, 1H; H_α D-Phe₅), 4.51 (m, 1H; H_α Leu₄), 4.48 (d, J = 11.4 Hz, 1H; CH₂ Benzyl), 4.36 (m, 1H; H_α Pro₆), 4.32 (q, J = 7.4 Hz, 1H; H_α Leu₉), 4.22 (t, J = 7.6 Hz, 1H; H_α Val₇), 4.14 (t, J = 8.2 Hz, 1H; H_α Val₂), 4.02 (d, J = 11.7 Hz, 1H; H₁ SAA₆), 3.65 (m, 1H; H_{6d}

SAA₆), 3.58 (m, 1H; H_{6d} Pro₆), 3.44 (m, 1H; H₅ SAA₆), 3.32 (m, 1H; H_{6u} SAA₆), 3.19 (td, J = 10.3, 4.4 Hz, 1H; H₄ SAA₆), 3.03 (dd, J = 12.7, 5.9 Hz, 1H; H_{βd} D-Phe₅), 2.94 (m, 3H; H_{βu} D-Phe₅, H_{βdu} Orn₃), 2.84 (m, 2H; H_{βdu} Orn₈), 2.60 (q, J = 8.4 Hz, 1H; H_{3u} Pro₆), 2.35 (m, 1H; H_{2d} SAA₆), 2.12–2.00 (m, 3H; H_{sd} SAA₆, H_β Val_{2,7}), 1.89 (m, 3H; H_{βdu} Pro₆, H_{βd} Orn₃), 1.80 (m, 2H; H_{βd} Orn₈), 1.67–1.51 (m, 8H; H_{βu,γdu} Orn, H_{γdu} Pro₆), 1.48–1.34 (m, 6H; H_{βdu,γ} Leu), 1.12 (m, 1H; H_{3u} SAA₆), 0.88 (d, J = 7.0 Hz, 3H; CH₃ Val₂), 0.86 (d, J = 7.1 Hz, 3H; CH₃ Val₂), 0.84 (d, J = 7.0 Hz, 3H; CH₃ Val₇), 0.82 (d, J = 5.3 Hz, 9H; CH₃ Leu₄, Val₇), 0.79 (d, J = 5.3 Hz, 6H; CH₃ Leu₉); ^{13}C NMR (151 MHz, $\text{H}_2\text{O}+\text{D}_2\text{O}$): δ = 174.92, 174.75, 174.43, 173.88, 173.41, 173.29, 173.10, 163.99, 163.75, 138.23, 136.34, 130.21, 129.90, 129.84, 129.58, 128.57, 118.27, 116.32, 78.89, 75.98, 72.96, 71.73, 67.54, 61.65, 59.70, 59.05, 55.22, 54.13, 53.39, 51.89, 48.15, 41.44, 40.97, 40.28, 40.23, 39.90, 36.76, 32.27, 32.14, 31.25, 30.36, 29.88, 28.87, 28.38, 25.39, 25.17, 24.47, 24.36, 23.27, 23.18, 22.74, 22.48, 19.69, 19.35, 18.82, 18.46 ppm; HRMS (ESI): m/z : calcd for $\text{C}_{60}\text{H}_{94}\text{N}_{11}\text{O}_{11}$: 1144.71288; found: 1144.71441 [$M+\text{H}$] $^+$; LCMS: R_t = 7.22 min, linear gradient 10 → 90% B in 13.5 min.; m/z : 1145.0 [$M+\text{H}$] $^+$.

Acknowledgements

This work was supported by the Leiden Institute of Chemistry. Assistance in performing NMR spectroscopic measurements and computational studies by C. Erkelens, A. W. M. Lefeber, and K. Babu is kindly acknowledged. We thank H. van den Elst for recording HRMS data and maintaining LCMS systems. We thank FIP and ESRF-Grenoble for provision of beam-time on beamlines BM30A and ID23–2, respectively. J.M.O. thanks the Xunta de Galicia and Spanish Ministry of Science and Innovation for “Ángeles Alvarinho” and “José Castillejo” fellowships, respectively. This work was funded by grant BFU2008-01588 to M.J.v.R. from the Spanish Ministry of Science and Innovation.

- [1] S. A. W. Gruner, E. Locardi, E. Lohof, H. Kessler, *Chem. Rev.* **2002**, *102*, 491–514.
- [2] a) F. Schweizer, *Angew. Chem.* **2002**, *114*, 240–264; *Angew. Chem. Int. Ed.* **2002**, *41*, 230–253; b) T. K. Chakraborty, S. Ghosh, S. Jayaprakash, *Curr. Med. Chem.* **2002**, *9*, 421–435; c) I. Velter, B. La Ferla, F. Nicotra, *J. Carbohydr. Chem.* **2006**, *25*, 97–138; d) J. L. J. Blanco, F. Ortega-Caballero, C. O. Mellet, J. M. G. Fernandez, *Beilstein J. Org. Chem.* **2010**, *6*, No. 20.
- [3] a) B. Aguilera, G. Siegal, H. S. Overkleeft, N. J. Meeuwenoord, F. Rutjes, J. C. M. van Hest, H. E. Schoemaker, G. A. van der Marel, J. H. van Boom, M. Overhand, *Eur. J. Org. Chem.* **2001**, 1541–1547; b) T. K. Chakraborty, D. Koley, R. Ravi, V. Krishnakumari, R. Nagaraj, A. C. Kunwar, *J. Org. Chem.* **2008**, *73*, 8731–8744; c) B. Lopez-Ortega, S. F. Jenkinson, T. D. W. Claridge, G. W. J. Fleet, *Tetrahedron: Asymmetry* **2008**, *19*, 976–983; d) R. Baron, D. Bakowies, W. F. van Gunsteren, *J. Pept. Sci.* **2005**, *11*, 74–84.
- [4] B. A. Mays, R. J. E. Stetz, M. P. Watterson, A. A. Edwards, C. W. G. Ansell, G. E. Tranter, G. W. J. Fleet, *Tetrahedron: Asymmetry* **2004**, *15*, 627–638.
- [5] M. D. P. Risseeuw, M. Overhand, G. W. J. Fleet, M. I. Simone, *Tetrahedron: Asymmetry* **2007**, *18*, 2001–2010.
- [6] E. G. von Roedern, H. Kessler, *Angew. Chem.* **1994**, *106*, 684–686; *Angew. Chem. Int. Ed. Engl.* **1994**, *33*, 687–689.
- [7] a) G. M. Grotenbreg, M. Kronemeijer, M. S. M. Timmer, F. El Oualid, R. M. van Well, M. Verdoes, E. Spalburg, P. A. V. van Hooft, A. J. de Neeling, D. Noort, J. H. van Boom, G. A. van der Marel, H. S. Overkleeft, M. Overhand, *J. Org. Chem.* **2004**, *69*, 7851–7859; b) V. V. Kapoerchan, E. Spalburg, A. J. de Neeling, R. H. Mars-Groenendijk, D. Noort, J. M. Otero, P. Ferraces-Casais, A. L. Llamas-Saiz, M. J. van Raaij, J. van Doorn, G. A. van der Marel, H. S. Overkleeft, M. Overhand, *Chem. Eur. J.* **2010**, *16*, 4259–4265.
- [8] G. F. Gause, M. G. Brazhnikova, *Nature* **1944**, *154*, 703.
- [9] M. Berditsch, S. Afonin, A. S. Ulrich, *Appl. Environ. Microbiol.* **2007**, *73*, 6620–6628.

- [10] a) D. C. Hodgkin, B. M. Oughton, *Biochem. J.* **1957**, *65*, 752–756; b) G. M. J. Schmidt, D. C. Hodgkin, B. M. Oughton, *Biochem. J.* **1957**, *65*, 744–750.
- [11] L. H. Kondejewski, S. W. Farmer, D. S. Wishart, R. E. W. Hancock, R. S. Hodges, *Int. J. Pept. Protein Res.* **1996**, *47*, 460–466.
- [12] C. J. Wadsten, C. A. Bertilsson, H. Sieradzki, S. Edstrom, *Arch. Oto-Rhino-Laryngol.* **1985**, *242*, 135–139.
- [13] a) G. M. Grotenbreg, M. S. M. Timmer, A. L. Llamas-Saiz, M. Verdoes, G. A. van der Marel, M. J. van Raaij, H. S. Overkleeft, M. Overhand, *J. Am. Chem. Soc.* **2004**, *126*, 3444–3446; b) G. M. Grotenbreg, A. E. M. Buizert, A. L. Llamas-Saiz, E. Spalburg, P. A. V. van Hooft, A. J. de Neeling, D. Noort, M. J. van Raaij, G. A. van der Marel, H. S. Overkleeft, M. Overhand, *J. Am. Chem. Soc.* **2006**, *128*, 7559–7565.
- [14] a) C. Solanas, B. G. de La Torre, M. Fernandez-Reyes, C. M. Santiveri, M. A. Jimenez, L. Rivas, A. I. Jimenez, D. Andreu, C. Cativiella, *J. Med. Chem.* **2010**, *53*, 4119–4129; b) C. Solanas, B. G. de La Torre, M. Fernandez-Reyes, C. M. Santiveri, M. A. Jimenez, L. Rivas, A. I. Jimenez, D. Andreu, C. Cativiella, *J. Med. Chem.* **2009**, *52*, 664–674; c) A. D. Knijnenburg, E. Spalburg, A. J. de Neeling, R. H. Mars-Groenendijk, D. Noort, G. M. Grotenbreg, G. A. van der Marel, H. S. Overkleeft, M. Overhand, *ChemMedChem* **2009**, *4*, 1976–1979.
- [15] A. W. Tuin, D. K. Palachanis, A. Buizert, G. M. Grotenbreg, E. Spalburg, A. J. de Neeling, R. H. Mars-Groenendijk, D. Noort, G. A. van der Marel, H. S. Overkleeft, M. Overhand, *Eur. J. Org. Chem.* **2009**, 4231–4241.
- [16] A. A. Edwards, G. W. J. Fleet, G. E. Tranter, *Chirality* **2006**, *18*, 265–272.
- [17] D. R. Witty, G. W. J. Fleet, K. Vogt, F. X. Wilson, Y. Wang, R. Storer, P. L. Myers, C. J. Wallis, *Tetrahedron Lett.* **1990**, *31*, 4787–4790.
- [18] O. Dahlman, P. J. Garegg, H. Mayer, S. Schramek, *Acta Chem. Scand. Ser. B* **1986**, *40*, 15–20.
- [19] H. S. Overkleeft, S. H. L. Verhelst, E. Pieterman, W. J. Meeuwenoord, M. Overhand, L. H. Cohen, G. A. van der Marel, J. H. van Boom, *Tetrahedron Lett.* **1999**, *40*, 4103–4106.
- [20] P. A. M. van der Klein, W. Filemon, G. H. Veeneman, G. A. van der Marel, J. H. van Boom, *J. Carbohydr. Chem.* **1992**, *11*, 837–848.
- [21] G. C. Chi, B. I. Seo, V. Nair, *Nucleosides Nucleotides Nucleic Acids* **2005**, *24*, 481–484.
- [22] C. Griesinger, R. R. Ernst, *J. Magn. Reson. (1969–1992)* **1987**, *75*, 261–271.
- [23] K. Wüthrich, *Nuclear Magnetic Resonance of Proteins and Nucleic Acids*, John Wiley & Sons, New York, **1986**.
- [24] A. Pardi, M. Billeter, K. Wüthrich, *J. Mol. Biol.* **1984**, *180*, 741–751.
- [25] a) A. J. Maynard, G. J. Sharman, M. S. Searle, *J. Am. Chem. Soc.* **1998**, *120*, 1996–2007; b) S. R. Griffiths-Jones, A. J. Maynard, M. S. Searle, *J. Mol. Biol.* **1999**, *292*, 1051–1069; c) the δ_{Ha} of the amino acid residues in GS are not significantly affected when using methanol instead of water as the solvent system. For the Orn residues, the random coil value of Lys is taken.
- [26] M. Kinoshita, Y. Okamoto, F. Hirata, *J. Am. Chem. Soc.* **2000**, *122*, 2773–2779.
- [27] a) R. M. van Well, L. Marinelli, C. Altona, K. Erkelens, G. Siegal, M. van Raaij, A. L. Llamas-Saiz, H. Kessler, E. Novellino, A. Lavencia, J. H. van Boom, M. Overhand, *J. Am. Chem. Soc.* **2003**, *125*, 10822–10829; b) T. Cierpicki, J. Otlewski, *J. Biomol. NMR* **2001**, *21*, 249–261.
- [28] D. S. Wishart, L. H. Kondejewski, P. D. Semchuk, C. M. Kay, R. S. Hodges, B. D. Sykes, in *Techniques in Protein Chemistry VI* (Ed: J. W. Crabb) Academic Press, Orlando, **1995**, pp. 451–458.
- [29] D. Neuhaus, M. P. Williamson, *The Nuclear Overhauser Effect in Structural and Conformational Analysis*, Wiley, New York, **1989**.
- [30] a) C. Altona in *Encyclopedia of NMR* (Eds.: D. M. Grant, R. K. Harris, Wiley, New York, **1996**, p. 4909; b) D. S. Wishart, B. D. Sykes, F. M. Richards, *J. Mol. Biol.* **1991**, *222*, 311–333; c) D. S. Wishart, B. D. Sykes, F. M. Richards, *Biochemistry* **1992**, *31*, 1647–1651; d) A. C. Gibbs, L. H. Kondejewski, W. Gronwald, A. M. Nip, R. S. Hodges, B. D. Sykes, D. S. Wishart, *Nat. Struct. Biol.* **1998**, *5*, 284–288.
- [31] D. F. Mierke, H. Kessler, *Biopolymers* **1993**, *33*, 1003–1017.
- [32] T. F. Havel, *Prog. Biophys. Mol. Biol.* **1991**, *56*, 43–78.
- [33] A. T. Hagler, S. Lifson, P. Dauber, *J. Am. Chem. Soc.* **1979**, *101*, 5122–5130.
- [34] A. L. Llamas-Saiz, G. M. Grotenbreg, M. Overhand, M. J. van Raaij, *Acta Crystallogr. Sect. D* **2007**, *63*, 401–407.
- [35] L. Wang, T. Oconnell, A. Tropsha, J. Hermans, *J. Mol. Biol.* **1996**, *262*, 283–293.
- [36] a) V. V. Kapoerchan, A. D. Knijnenburg, M. Niamat, E. Spalburg, A. J. de Neeling, P. H. Nibbering, R. H. Mars-Groenendijk, D. Noort, J. M. Otero, A. L. Llamas-Saiz, M. J. Van Raaij, G. A. van der Marel, H. S. Overkleeft, M. Overhand, *Chem. Eur. J.* **2010**, *16*, 12174–12181; b) L. H. Kondejewski, M. Jelokhani-Niaraki, S. W. Farmer, B. Lix, C. M. Kay, B. D. Sykes, R. E. W. Hancock, R. S. Hodges, *J. Biol. Chem.* **1999**, *274*, 13181–13192; c) D. L. Lee, J. P. S. Powers, K. Pfelegerl, M. L. Vasil, R. E. W. Hancock, R. S. Hodges, *J. Pept. Res.* **2004**, *63*, 69–84; d) E. J. Prenner, M. Kiricsi, M. Jelokhani-Niaraki, R. Lewis, R. S. Hodges, R. N. McElhaney, *J. Biol. Chem.* **2005**, *280*, 2002–2011; e) A. D. Knijnenburg, V. V. Kapoerchan, E. Spalburg, A. J. de Neeling, R. H. Mars-Groenendijk, D. Noort, G. A. van der Marel, H. S. Overkleeft, M. Overhand, *Bioorg. Med. Chem.* **2010**, *18*, 8403–8409.
- [37] a) E. F. Haney, S. Nathoo, H. J. Vogel, E. J. Prenner, *Chem. Phys. Lipids* **2010**, *163*, 82–93; E. J. Prenner, R. Lewis, R. N. McElhaney, *Biochim. Biophys. Acta Biomembr.* **1999**, *1462*, 201–221; b) Md. Ashrafuzzaman, O. S. Andersen, R. N. McElhaney, *Biochim. Biophys. Acta Biomembr.* **2008**, *1778*, 2814–2822; c) M. Jelokhani-Niaraki, R. S. Hodges, J. E. Meissner, U. E. Hassenstein, L. Wheaton, *Biophys. J.* **2008**, *95*, 3306–3321; d) S. Semrau, M. W. L. Monster, M. van der Knaap, B. I. Florea, T. Schmidt, M. Overhand, *Biochim. Biophys. Acta Biomembr.* **2010**, *1798*, 2033–2039.
- [38] A. G. W. Leslie, H. R. Powell, G. Winter, O. Svensson, D. Spruce, S. McSweeney, D. Love, S. Kinder, E. Duke, C. Nave, *Acta Crystallogr. Sect. D* **2002**, *58*, 1924–1928.
- [39] W. Kabsch, *J. Appl. Crystallogr.* **1993**, *26*, 795–800.
- [40] G. M. Sheldrick, *Acta Crystallogr. Sect. A* **2008**, *64*, 112–122.
- [41] L. J. Farrugia, *J. Appl. Crystallogr.* **1999**, *32*, 837–838.

Received: October 7, 2010
Published online: March 1, 2011